

A biodegradable and biocompatible gecko-inspired tissue adhesive

Alborz Mahdavi*, Lino Ferreira*[†], Cathryn Sundback*[‡], Jason W. Nichol[¶], Edwin P. Chan[¶], David J. D. Carter[¶], Chris J. Bettinger[¶], Siamrut Patanavanich*, Loice Chignozha*, Eli Ben-Joseph*, Alex Galakatos*, Howard Pryor*[‡], Irina Pomerantseva*[‡], Peter T. Masiakos*[‡], William Faquin*[‡], Andreas Zumbuehl*[‡], Seungpyo Hong*, Jeffrey Borenstein[¶], Joseph Vacanti*[‡], Robert Langer*[¶], and Jeffrey M. Karp*[¶]

*Department of Chemical Engineering, Massachusetts Institute of Technology, Cambridge, MA 02139-4307; [†]Center of Neurosciences and Cell Biology, University of Coimbra, and Biocant Biotechnology Innovation Center, 3060-197 Cantanhede, Portugal; [‡]Center for Regenerative Medicine and Departments of [¶]Pediatric Surgery and [¶]Pathology, Massachusetts General Hospital, Boston, MA 02114; [§]Harvard Medical School, Boston, MA 02115; [¶]Harvard–Massachusetts Institute of Technology, Division of Health Science and Technology, Cambridge, MA 02139; [¶]The Charles Stark Draper Laboratory, Cambridge, MA 02139-3563; [‡]Biozentrum, University of Basel, Klingelbergstrasse 50/70, 4056 Basel, Switzerland; and [¶]Health Sciences and Technology, Center for Biomedical Engineering, Brigham and Women's Hospital, Boston, MA 02115

Contributed by Robert Langer, December 26, 2007 (sent for review November 30, 2007)

There is a significant medical need for tough biodegradable polymer adhesives that can adapt to or recover from various mechanical deformations while remaining strongly attached to the underlying tissue. We approached this problem by using a polymer poly(glycerol-co-sebacate acrylate) and modifying the surface to mimic the nanotopography of gecko feet, which allows attachment to vertical surfaces. Translation of existing gecko-inspired adhesives for medical applications is complex, as multiple parameters must be optimized, including: biocompatibility, biodegradation, strong adhesive tissue bonding, as well as compliance and conformability to tissue surfaces. Ideally these adhesives would also have the ability to deliver drugs or growth factors to promote healing. As a first demonstration, we have created a gecko-inspired tissue adhesive from a biocompatible and biodegradable elastomer combined with a thin tissue-reactive biocompatible surface coating. Tissue adhesion was optimized by varying dimensions of the nanoscale pillars, including the ratio of tip diameter to pitch and the ratio of tip diameter to base diameter. Coating these nanomolded pillars of biodegradable elastomers with a thin layer of oxidized dextran significantly increased the interfacial adhesion strength on porcine intestine tissue *in vitro* and in the rat abdominal subfascial *in vivo* environment. This gecko-inspired medical adhesive may have potential applications for sealing wounds and for replacement or augmentation of sutures or staples.

chemical cross-link | medical adhesive | nanotopography | surgical suture

The ability of gecko feet to adhere to vertical and inverted surfaces (1–7) has prompted this study to assess the impact of gecko-like morphology on the properties of chemical reaction based tissue adhesives. Fibrillar arrays, which cover the bottom of gecko feet, maximize the interfacial adhesion to surfaces. Specifically, the adhesive footpads are decorated with a dense array of fibrils (setae); each seta has numerous terminal projections (spatulae) that are 200–500 nm in length (1, 2). The combination of van der Waals (3) and capillary forces (5) controls the adhesion of these spatulae to surfaces. Based on this understanding, synthetic gecko adhesives (8, 9) have been developed that recapitulate these two gecko adhesion features: (i) adhesion in a dry environment without a chemical “glue” and (ii) a fibrillar design that enhances interface compliance and conformability to surfaces with a variety of roughness.

Despite the growing interest in developing gecko-inspired medical adhesives, only a single adhesive has been optimized for a wet tissue-like environment. Specifically, important work from P. Messersmith's group has demonstrated a synthetic gecko adhesive that is effective under water with reversible noncovalent bonding to inorganic surfaces (10). However, adhesives for medical applications require strong irreversible bonds to organic substrates to avoid

disruption by the movement of underlying or nearby tissues. Furthermore, the bond strengths of experimental adhesives must be tested under physiological conditions. To our knowledge, *in vivo* studies have not been reported with gecko-inspired surfaces. The bond strengths of gecko-inspired adhesives are typically evaluated through submicrometer atomic force microscopy measurements, which may not be predictive of macroscopic patch performance.

In this study, a gecko-inspired tissue adhesive was developed that is elastomeric, biocompatible, and biodegradable. This adhesive is based on poly(glycerol sebacate acrylate) (PGSA), a tough biodegradable elastomer (11, 12) with elastic and biodegradation properties that can be tuned for specific tissue applications and can be easily doped with growth factors or drugs (11). Through combined morphology and chemistry effects, we have demonstrated a biocompatible tissue adhesive with promising covalent cross-linking to wet tissue. This tape-based tissue adhesive platform may have application in medical therapies ranging from suture/staple replacements/supplements; waterproof sealants for hollow organ anastomoses; mesh grafts to treat hernias, ulcers, and burns; and hemostatic wound dressings.

Results and Discussion

Development of Biodegradable Elastomeric Gecko-Inspired Nanopatterns. A fabrication procedure for manufacturing tissue adhesives was developed that avoids high-temperature and harsh chemical conditions that is amenable to a variety of materials. Silicon templates were prepared by using the microfabrication techniques of photolithography and reactive ion etching. To create the nanopattern (Fig. 1a), linear PGSA polymer was cast on nanomold cavities, without high vacuum, and cured by UV light in <5 min at room temperature. To determine the impact of pattern dimensions on PGSA adhesive properties, pillar arrays were patterned in PGSA with tip pillar diameters ranging from ≈100 nm to 1 μm and pillar heights from ≈0.8 to ≈3 μm (Fig. 1b).

The adhesive strength of gecko surfaces to wet substrates depends on the hydrophobic and hydrophilic nature of the substrates and is significantly lower than on dry substrates (3, 6). A recent innovative study for gecko adhesives that work under wet conditions

Author contributions: A.M. and L.F. contributed equally to this work; A.M., L.F., C.S., J.W.N., D.J.D.C., C.J.B., A.Z., S.H., J.B., J.V., R.L., and J.M.K. designed research; A.M., L.F., C.S., J.W.N., D.J.D.C., S.P., L.C., E.B.J., A.G., H.P., I.P., and P.T.M. performed research; A.M., L.F., C.S., J.W.N., E.P.C., D.J.D.C., W.F., and J.M.K. analyzed data; and A.M., L.F., C.S., E.P.C., R.L., and J.M.K. wrote the paper.

§§To whom correspondence may be addressed. E-mail: rlander@mit.edu or jkarp@rics.bwh.harvard.edu.

The authors declare no conflict of interest.

This article contains supporting information online at www.pnas.org/cgi/content/full/0712117105/DC1.

© 2008 by The National Academy of Sciences of the USA

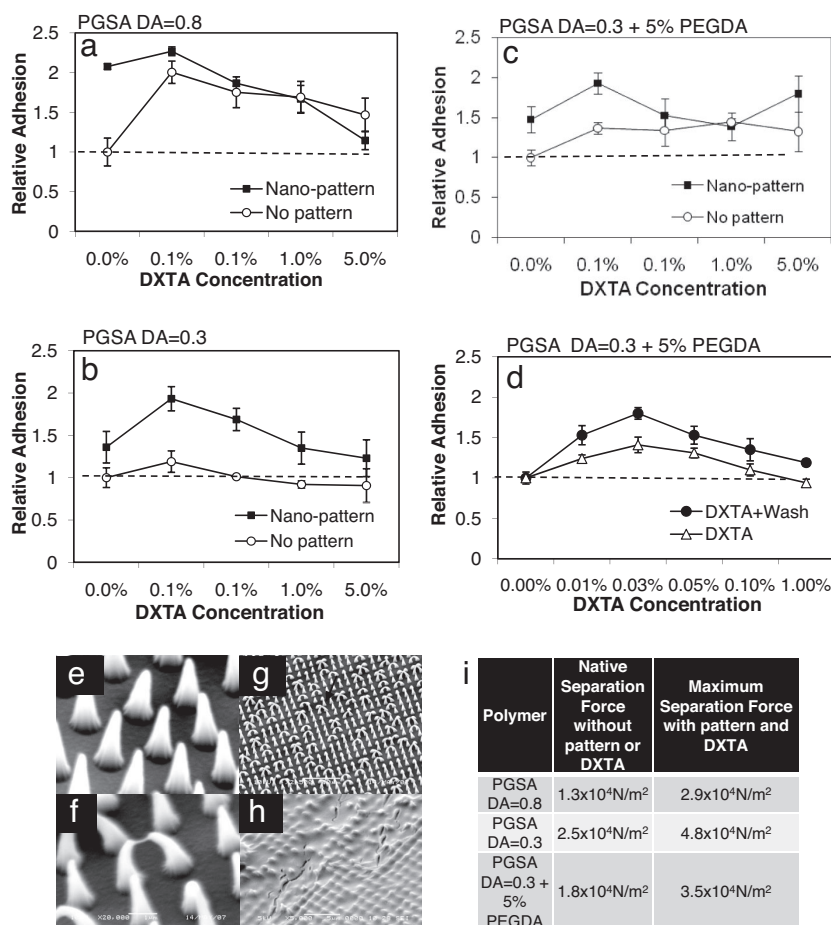


Fig. 3. DXTA coating of nanopatterned PGSA polymer improves tissue adhesion *in vitro*. (a–c) Relative adhesion of nanopatterned vs. unpatterned PGSA polymer to porcine tissue slides as a function of DXTA surface coating concentration. A represents PGSA DA = 0.8, B is PGSA DA = 0.3 with 5% PEGDA, and C is PGSA DA = 0.3. Data were normalized to the unpatterned DA = 0.8 PGSA polymer without DXTA coating. (d) Normalized adhesion results of the PGSA DA = 0.3 with 5% PEG DA shows the effect of washing on improving adhesion at various DXTA concentrations. (e) Nanopatterned PGSA polymer after surface spin coating with water as control. (f and g) Nanopatterned PGSA after surface spin coating with 0.05% DXTA solution shows adhesion of neighboring pillar tips. The black arrow indicates how DXTA polymer may cause neighboring pillar tips to stick together. (h) Five percent DXTA completely obstructed the underlying nanopattern. (i) The baseline adhesion and maximum values obtained for each material used.

that are known to degrade polyesters (17). After 8 days of degradation, SEM images of the patterns as shown in Fig. 4b revealed that pillars and bulk underlying the PGSA material have started to degrade. In contrast, no observable degradation of pillars occurred during the 8-day experiment in the PGSA DA = 0.8 and PGSA DA = 0.3 with 5% PGDA formulations (data not shown).

Biocompatibility of Gecko Tissue Tape. With the purpose of evaluating the effect of nanopatterned surfaces and the DXTA coating on tissue biocompatibility and adhesiveness, we implanted 1-cm² adhesive patches in the subfascial environment overlying the rectus muscle of rats, selected for its clinical relevance. As shown in Fig. 4c, flexible adhesive gecko tapes were cut into square patches and inserted into fascial flaps on the underlying rectus muscle with the nanopattern oriented outward toward the fascia. Weight-loss measurements of gecko patterns after 1-week implantation showed a negligible difference between the 0.3 and 0.3 + PEGDA PGSA patterns (Fig. 4d). In accordance with our previous findings (11), the PGSA with higher DA (0.8) had a smaller weight loss, which is indicative of slower degradation.

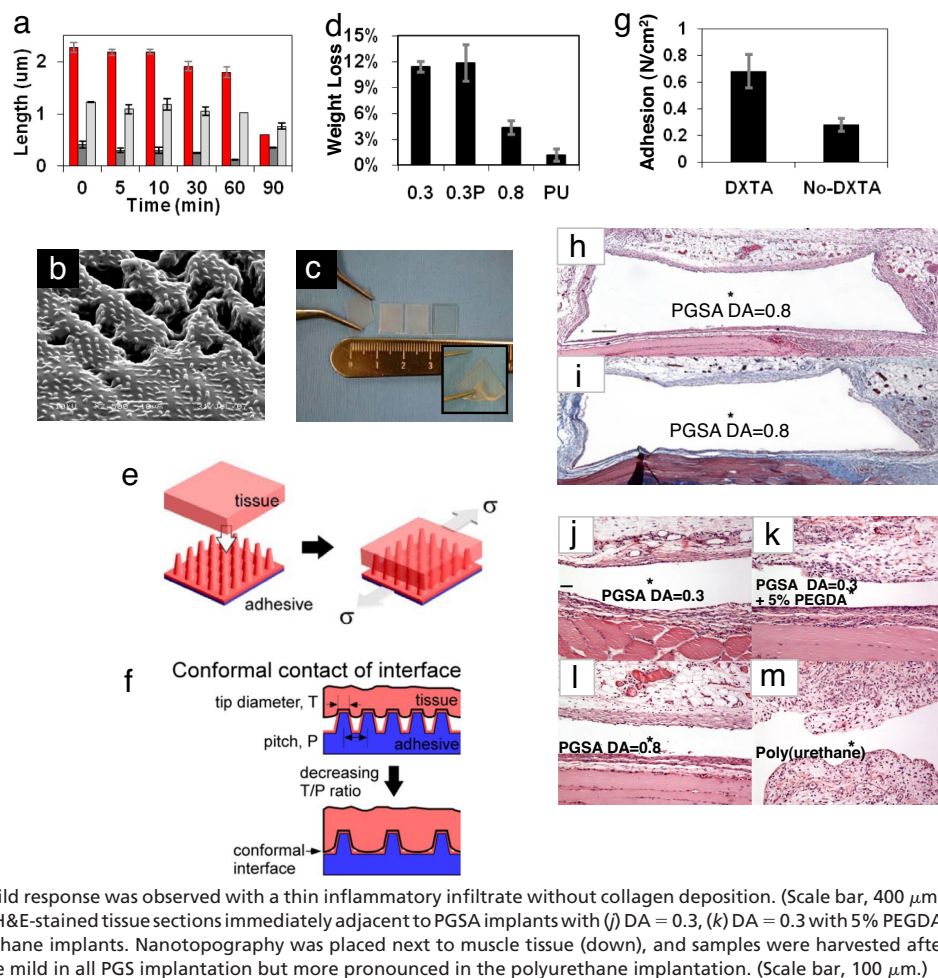
Adhesive strength was determined by using a test apparatus shown in Fig. 4e, where explanted tissue containing the adherent patch was fixed on a glass slide, and a defined mechanical shear force was applied. As the results in Fig. 1c and d suggest, a decrease in the tip diameter to pitch ratio (T/P) actually leads to an enhancement in adhesion. In other words, maximum enhancement occurs for the pattern with the lowest density of pillars. This observation is counterintuitive, because previous work on patterned adhesion demonstrated that enhancement is based on the mechanism of contact line splitting that requires maximizing the pillar density (18). However, our materials are unique in that the

pillars are interfacing with another soft compliant surface, i.e., the deformable tissue. Although additional experimental results are necessary for confirmation, one possible means of enhancement is associated with the enhanced conformal contact between the tissue and PGSA patterned adhesive. As Fig. 4d illustrates, within a narrow range the tissue can better conform to the patterned adhesive surface when the distance between pillars is sufficiently large and the tip diameter sufficiently low (Fig. 4f). Otherwise, the tissue cannot conform to the area between the pillars and reduces the interfacial contact area (Fig. 4f). Hence, for a constant pillar height, the ratio T/P is an empirical descriptor that describes the ability for the tissue interface to conform to the patterned surface and increase the interfacial contact area.

To determine whether improved adhesion from DXTA coating is maintained over time, adhesion of the gecko patterns was measured after 48 h of implantation. As shown in Fig. 4g, the adhesive strength of DXTA-coated gecko patterns was >2-fold higher than samples without the DXTA coating.

To assess the effect of polymer composition and nanotopography on tissue response, disks of patterned PGSA polymer were implanted subcutaneously in the backs of rats for 7 days. In agreement with reported observations (12, 19), the tissue response was mild (Fig. 4h and i) and did not depend on PGSA nanotopography or formulation (Fig. 4j–m). As reported by a blinded pathologist, a thin inflammatory infiltrate layer with little vascularization encircled the implant cavity, similar to previous implantation studies. No giant cell reaction was observed. The chronic inflammation to nonresorbable polyurethane (Fig. 4m), which was used as a control, was more pronounced, because the cellular infiltrate surrounding the implant had distinctive papillary architecture with increased vascularity and edema. The tissue response was not assessed in the

Fig. 4. *In vivo* characterization of synthetic tissue tape. (a) Time-lapsed optical profilometry measurements of pillar dimensions during *in vitro* degradation in 1 M sodium hydroxide solution (color scheme as in Fig. 1b). (b) SEM image of PGSA DA = 0.3 gecko-patterned surface shows presence of pillars after eight days of *in vitro* degradation under physiological conditions in 1 units/ml of cholesterol esterase enzyme. (Scale bar, 10 μm .) (c) Representative image of 1-cm² patches of gecko tissue tape, which were used for *in vivo* experiments. Elasticity of the samples is demonstrated through stretching and bending of the samples using forceps (*Inset*). (d) Weight-loss measurements after 1 week implantation of samples with different compositions of PGSA and a polyurethane control (PU). (e) Shear adhesion tests were performed on explanted tissue. (f) Within a narrow range, patterned adhesives may exhibit enhanced surface area of contact with tissue when the distance between pillars are sufficiently large and the tip diameter sufficiently low. (g) *In vivo* adhesion strength of DXTA-coated PGSA DA = 0.8 samples after being implanted for 48 h. (h and i) Tissue response to nanopatterned PGSA disks with DA = 0.8, s.c. implanted in the rat dorsum. Low-magnification photomicrographs of (h) H&E and (i) Masson's trichrome-stained tissue sections immediately adjacent to PGSA implants. PGSA implants formerly occupied open spaces denoted by *. Nanotopography was placed next to muscle tissue (down), and samples were harvested after 1-week implantation. A mild response was observed with a thin inflammatory infiltrate without collagen deposition. (Scale bar, 400 μm .) (j–m) High-magnification photomicrographs of H&E-stained tissue sections immediately adjacent to PGSA implants with (j) DA = 0.3, (k) DA = 0.3 with 5% PEGDA, and (l) DA = 0.8 and (m) unpatterned polyurethane implants. Nanotopography was placed next to muscle tissue (down), and samples were harvested after 1-week implantation. The tissue responses were mild in all PGS implantation but more pronounced in the polyurethane implantation. (Scale bar, 100 μm .)



functional tests for the materials that were implanted in the preperitoneal space. This functional model provided the benefit of evaluating the adhesiveness of the material in contact with two unique tissue surfaces. Extensive surgical manipulation of the tissue was required, which induced some expected muscle degradation with marked fibroblastic proliferation that masked any inflammatory response to the implanted materials. Taken together, these results suggest that introduction of gecko nanopatterned substrates or the DXTA coating on the surface of the PGSA polymer did not result in an increased tissue response to the implant. Therefore, a general strategy of using a judicious choice of surface patterning with tissue-compatible surface chemistry can provide an effective means to achieve tissue adhesion.

The mechanism of enhancement in our materials is based on mechanical interlocking with the tissue. Compared with the gecko and other gecko-based adhesives, which are based on spatular surface contact and weak reversible adhesion, strong single-use tissue adhesives require additional mechanisms, such as mechanical interlocking and covalent chemistry. Unlike the gecko, permanent deformation of the interface may occur during debonding. Although this mechanism differs significantly from that of the gecko, i.e., contact line splitting, the basic principles of adhesion enhancement are similar: intelligent design of a patterned interface to enhance interfacial contact.

Conclusions

Through screening a variety of nanopatterned morphologies and exploring the cumulative effects of surface morphology with chemistry using a biocompatible and biodegradable elastomer, we have

developed a tissue-compliant synthetic gecko-inspired adhesive that may be useful for a range of medical applications. *In vivo* characterization of implanted gecko tapes demonstrated minimal tissue response. Therefore, this strategy may provide an effective method for the development of tissue adhesives that can potentially provide a platform for many practical and useful additions to the surgical armamentarium.

Materials and Methods

Nanomolding of PGSA Polymer. Nanomolds were fabricated by using photolithography followed by reactive ion etching of an oxide layer on a silicon wafer. Oxidation of silicon wafers and incorporation and development of resist films are described in *SI Text*. The photomask was fabricated by Photronics. The wafer was then ashed in a March barrel asher for 30 seconds at 55 W in a 250-mTorr oxygen plasma. Reactive ion etching was then used to transfer the pattern of hole arrays into the oxide layer to form the mold. We used a Surface Technology Systems (STS) Multiplex Reactive ion etching with gas flows of 14.4 standard cubic centimeters per minute (sccm) of CHF_3 and 1.6 sccm of CF_4 at 20-mTorr pressure. An oxide etch rate of ≈ 2.8 nm/second was achieved by using 200 W of radiofrequency power. Three mold depths were targeted by controlling the etch time, with approximate depths of 1, 2, and 3.5 μm . After etching, the resist layer was removed by sequential rinse in acetone and SVC-12 (Microchem) for 30 min each and EKC-270 stripper (DuPont) for 2.5 h followed by a 10-min rinse with deionized water and spin drying. The etched oxide depth was measured by profilometry on a Tencor Alpha-Step-IQ. To develop patterned polymer surfaces, PGSA prepolymer was poured onto silicon molds without applying vacuuming and was UV-cured as described (11). The macroscopic film thicknesses for all of the polymer adhesives were kept constant at 0.94 ± 0.03 mm.

Shear Adhesion Tests. Shear adhesion tests were performed on the polymer surfaces using an Electroforce ELF 3200 mechanical tester (Bose-Enduratec) con-

trolled by WinTest software (Ver. 2.51) using custom-fabricated stainless steel tissue grips and a 250-g load cell (model 31-1435-03; Sensotech). This test of shear resistance provided a measure of the ability of the patterns to resist lateral movements on tissue once immobilized. To test adhesion, 4-mm discs of the polymer were cut out of patterns using a dermal biopsy punch (Miltex Instrument) and glued to a glass slide to provide a flat adhesive surface with well defined area. Porcine intestine tissue was cut into 2×2 -cm sections and glued to a glass slide using cyanoacrylate glue, and the outer surface of the intestine tissue was used for adhesion tests. The sample and tissue slides were positioned parallel to each other to provide contact between the tissue and patterned polymer sample. The position of the test samples was identical for all samples to minimize sample-to-sample variance in the initial contact or preload force. Upon initiation of the adhesion test, the tissue slide was displaced at a rate of 8 mm/min while the force was recorded.

Synthesis and Characterization of DXTA. DXTA was synthesized as described (20) (*SI Text*). The DXTA solution was spin-coated on the surface of the PGSA gecko pattern using a speed of 4,000 rpm, which was determined to be optimal for a uniform surface coating. DXTA hydrogels have an elastic modulus between 20 and 60 kPa, depending on the degree of cross-linking as described (21).

XPS and FTIR Analysis. XPS and FTIR measurements were carried out on an Axis Ultra spectrometer (Kratos Analytical) and a Nicolet Magna 860 FTIR instrument, respectively. Please see *SI Text* for the operating conditions.

In Vivo Characterization of Implanted Gecko Tissue Tape. Surgical procedures. All surgical procedures were approved by the Institutional Animal Care and Use Committee of the Massachusetts General Hospital and performed according to the National Institutes of Health Guidelines for the Care and Use of Laboratory Animals. See *SI Text* for details.

Biocompatibility studies. The tissue response was determined for nanopatterned PGSA materials (DA = 0.3, DA = 0.3 with 5% PEGDA, and DA = 0.8) and the control material, unpatterned nonresorbable polyurethane. For each PGSA formulation, 5-mm-diameter disks were punched from polymer sheets of 1.1-mm thickness using dermal biopsy punches (Acuderm, Acu-Punch) and dried at 60°C at 50 torr for 48 h and disinfected by UV light. Disks were s.c. implanted into pockets on the backs of five Wistar rats ($n = 8$ for each PGSA formulation; $n = 6$ for polyurethane). A small incision was made in the dorsal midline of each animal. Six small s.c. pockets deep inside the loose areolar tissue were developed using blunt dissection bilaterally over the scapular and the *latissimus dorsi* regions and

caudal to the pelvic brim. One sterile PGSA disk was inserted into each pocket, with the nanopattern facing the muscle, and each incision was closed with 2–0 silk sutures. One week after implantation, the rats were killed and samples located by palpation. Each PGS disk was excised with all associated surrounding dermal and muscle tissues.

Functional adhesion studies. Tissue adhesion of DXT-coated nanotextured 0.8 acrylation PGS samples was evaluated in the subfascial environment. A small incision was made in the ventral midline of each animal ($n = 7$). Dissection was carried down to the linea alba, and all loose areolar tissue was gently swept off the abdominal wall using damp gauze. After identifying the fascia, a small incision parallel to the linea alba was made bilaterally in the ventral aspect of the rectus sheath. A small fascial flap was developed using a blunt dissection technique on each side of the incision. A sample (1×1 cm, 1.1-mm thick) was placed in each flap on the exposed underlying rectus muscle with the nanopattern oriented outward toward the fascia; one nanopatterned/DXT-coated sample and one nanopatterned/uncoated sample were inserted into each animal. The overlying tissues were reapproximated, and the skin was closed with 2–0 silk sutures. Rats were killed after 48 h for adhesive testing. After shaving, the entire abdominal wall was removed, and the samples were identified by palpation. Each explant was excised from the abdominal wall with associated surrounding tissues from the dermis to the underlying muscle layer. Samples for adhesion testing were immersed in sterile saline and tested immediately after removal. The samples explanted at 7 d ($n = 3$) were prepared for histologic analysis.

PGSA explantation. For weight loss, the PGSA explants were carefully dissected from the surrounding tissue and rinsed in distilled water, dried at 60°C for 48 h at 50 torr vacuum, and weighed. For histological evaluation, the tissue surrounding the implant was carefully trimmed ($2 \times 2 \times 0.5$ cm), and both the tissue and sample were fixed in 10% buffered formalin. After 3 days, the tissue samples were cut in half, the capsules were incised, and the polymer disks were removed. Tissue was cut into 3-mm-wide sections and embedded in paraffin. Sections (6- μ m thick) were stained with H&E and Masson's trichrome and analyzed for the degree of inflammation and fibrosis. The tissue response was characterized based on the level of neutrophils, lymphocytes, macrophages, and giant cells. Fibrosis was identified primarily by collagen deposition.

ACKNOWLEDGMENTS. We thank Professor Lisa Freed for use of her ELF 3200 mechanical tester. This work was supported by National Institutes of Health Grant DE013023 and National Science Foundation Grant NIRT 0609182. This work was also supported by the Materials Research Science and Engineering Program of the National Science Foundation under award number DMR 02-1328 and the Massachusetts Institute of Technology–Portugal (focus in bioengineering). C.J.B. was supported by a Charles Stark Draper Laboratory Fellowship.

- Autumn K, Liang YA, Hsieh ST, Zesch W, Chan WP, et al. (2000) Adhesive force of a single gecko foot-hair. *Nature* 405:681–685.
- Pennisi E (2000) Biomechanics. Geckos climb by the hairs of their toes. *Science* 288:1717–1718.
- Autumn K, Sitti M, Liang YA, Peattie AM, Hansen WR, et al. (2002) Evidence for van der Waals adhesion in gecko setae. *Proc Natl Acad Sci USA* 99:12252–12256.
- Hansen WR, Autumn K (2005) Evidence for self-cleaning in gecko setae. *Proc Natl Acad Sci USA* 102:385–389.
- Sun W, Neuzil P, Kustandi TS, Oh S, Samper VD (2005) The nature of the gecko lizard adhesive force. *Biophys J* 89:14–17.
- Huber G, Mantz H, Spolenak R, Mecke K, Jacobs K, et al. (2005) Evidence for capillarity contributions to gecko adhesion from single spatula nanomechanical measurements. *Proc Natl Acad Sci USA* 102:16293–16296.
- Autumn K, Hansen W (2006) Ultrahydrophobicity indicates a non-adhesive default state in gecko setae. *J Comp Physiol* 192:1205–1212.
- Geim AK, Dubonos SV, Grigorieva IV, Novoselov KS, Zhukov AA, Shapoval SY (2003) Microfabricated adhesive mimicking gecko foot-hair. *Nat Mater* 2:461–463.
- Crosby AJ, Hageman M, Duncan A (2005) Controlling polymer adhesion with “pancakes”. *Langmuir* 21:11738–11743.
- Lee H, Lee BP, Messersmith PB (2007) A reversible wet/dry adhesive inspired by mussels and geckos. *Nature* 448:338–341.
- Nijst CL, Bruggeman JP, Karp JM, Ferreira L, Zumbuehl A, et al. (2007) Synthesis and characterization of photocurable elastomers from poly(glycerol-co-sebacate). *Biomacromolecules* 8:3067–3073.
- Wang Y, Ameer GA, Sheppard BJ, Langer R (2002) A tough biodegradable elastomer. *Nat Biotechnol* 20:602–606.
- Autumn K, Dittmore A, Santos D, Spenko M, Cutkosky M (2006) Frictional adhesion: a new angle on gecko attachment. *J Exp Biol* 209:3569–3579.
- Wang DA, Varghese S, Sharma B, Strehin I, Fermanian S, Fairbrother DH, Cascio B, Elisseeff JH (2007) Multifunctional chondroitin sulphate for cartilage tissue-biomaterial integration. *Nat Mater* 6:385–392.
- Mo X, Iwata H, Matsuda S, Ikada Y (2000) Soft tissue adhesive composed of modified gelatin and polysaccharides. *J Biomater Sci Polym Ed* 11:341–351.
- Somani BL, Khanade J, Sinha R (1987) A modified anthrone-sulfuric acid method for the determination of fructose in the presence of certain proteins. *Anal Biochem* 167:327–330.
- Santerre JP, Labow RS (1997) The effect of hard segment size on the hydrolytic stability of polyether-urea-urethanes when exposed to cholesterol esterase. *J Biomed Mat Res* 36:223–232.
- Chan E, Greiner C, Arzt E, Crosby A (2007) Design model systems for enhanced adhesion. *MRS Bull* 32:496–503.
- Sundback CA, Shyu JY, Wang Y, Faquin WC, Langer RS, Vacanti JP, Hadlock TA (2005) Biocompatibility analysis of poly(glycerol sebacate) as a nerve guide material. *Biomaterials* 26:5454–5464.
- Maia J, Ferreira L, Carvalho R, Ramos MA, Gil MH (2005) Synthesis and characterization of new injectable and degradable dextran-based hydrogels. *Polymer* 46:9604–9614.
- Ferreira L, Gil MH, Dordick JS (2002) Enzymatic synthesis of dextran-containing hydrogels. *Biomaterials* 23:3957–3967.